

## 13 Thermoelectric Coolers

A. Chuchra\* and T. Stevenson†

### Introduction

Thermoelectric coolers (TECs) are miniature solid-state heat pumps capable of providing localized cooling to devices that require cold temperatures for proper operation. Before 1990, their use was confined to unique situations, generally in laboratories or other engineered environments. Throughout the 1990s, however, thermoelectrically cooled devices became somewhat common in everyday terrestrial and commercial applications. Notable examples include six-pack-sized minirefrigerators for automotive and marine use and night-vision devices. TECs in space have also become relatively common; they cool low noise amplifiers (LNAs), star trackers, and IR (infrared) sensors. Table 13.1 lists spaceborne TECs.

### Background

TECs provide cooling via the Peltier effect, which is the cooling that results from the passage of an electric current through a junction formed by dissimilar metals. (Note: The Peltier effect is the inverse of the Seebeck effect, the basis for common thermocouples—in the Seebeck effect, a [temperature-varying] voltage results from the junction of dissimilar metals.) The simplest TEC consists of two semiconductors, one *p*-type and one *n*-type (one “couple”), connected by a metallic conductor, as depicted schematically in Fig. 13.1. Heat is pumped from the cold junction to the hot junction. The net cooling is diminished by the effects of Joulean losses generated by the current, and heat conduction through semiconductor material from the hot to the cold junction. Semiconductors, principally bismuth telluride ( $\text{Bi}_2\text{Te}_3$ ), have made these devices practical. Prior to the advent of such semiconductors, parasitic conduction through metal elements largely negated any useful cooling.

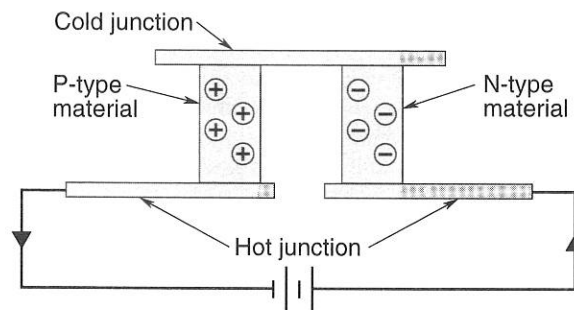


Fig. 13.1. Peltier thermoelectric couple.

\*Swales Aerospace, Beltsville, Maryland.

†University of Leicester, Leicester, United Kingdom.

Table 13.1. Survey of Spaceborne TECs

Spacecraft or Mission	Instrument/Component	Institution	Launch	No. of Stages	Parallel TECs	Cold Temp. (°C)	Rejection Temp. (°C)	Net Cooling (Tot.) (W)	Input Power (Tot.) (W)	
Satcom K Various	CLNA	RCA Astro	1985	4	Single	-50	15	0.79	8.0	
	Star tracker	Ball	Many for 2 decades	1	Single	0	20	1.8	1.7	
Hubble Space Telescope	STIS	Ball, GSFC	1997	4	Single	-80	20	0.3	17.7	
Hubble Space Telescope	NICMOS	Ball, UAZ, GSFC	1997	3	Dual	-73	10	0.25	10.75	
FUSE	Fine error sensor (star sensor)	ComDev, CSA, JHU-APL	1999	2	3	Dual	-47	5	0.6	2.4
					Single	-32	-10 to 0	2 (typ) 5 (max)		
Future missions										
Hubble Space Telescope	Advanced camera	Ball, JHU-APL	2003	2	Quad	-35	24	1.0	9	
					4	Single	-77	24	0.4	16.6
Swift	XRT	Univ. of Leicester	2003	4	4	Single	-81	24	0.3	15.5
					5	Single	-95 to 105	<-38	-0.1	4 to 5
Hubble Space Telescope	Wide field camera III	Ball, GSFC	2004	1	TBD	TBD	TBD	TBD	TBD	
					2	Quad	-55	-5	0.8	9
Mercury Messenger	MLA	GSFC, APL	2004	4	Dual	-83	-5	0.2	8.8	
					6	Single	-123	-35	0.028	12
				1	Single	10 to 25	10 to 25	0.6	0.6	

Vendors supply TEC modules as single-stage or multistage assemblies. A stage generally contains many elements electrically joined in series, with all cold junctions soldered to metallization on one ceramic plate and all hot junctions soldered to the opposite ceramic plate. Vendors can select the number of stages, the number of couples, and the geometry of the  $p$  or  $n$  post to optimize the coefficient of performance (COP). The COP is the useful cooling divided by the input power to the TEC. TECs with low COPs consume more power than is optimal and produce excessive waste heat. The exact temperature difference at which use of multistage TECs becomes more efficient than use of single-stage devices is not generally agreed upon. However, space applications have favored multistage TECs where the desired temperature difference exceeded the 25–40°C range. The shape of a multistage TEC resembles that of a multitiered wedding cake, with the upper layer representing the cold stage and the base layer representing the hot stage. Each stage needs to be larger than the one above it, to handle progressively larger amounts of waste heat; hence the cascading shape. This geometry also stems from the need to minimize the parasitic thermal coupling between stages.

For space application, TECs have the advantages of simplicity, reliability, compactness, low mass, and noiseless, vibrationless operation. Unlike common heat pumps (compression/expansion-based and Stirling cycle), these devices have no moving parts. Their use in spacecraft is limited by their relatively low COP, particularly with large temperature differences. Because of their limited efficiency, they are best suited to situations with modest heat loads, cold temperatures not below 150 K, and hot-to-cold-side differences not exceeding 100°C. Other cooling methodologies are generally better suited (more efficient) for applications with greater heat loads or larger temperature-difference requirements. Figure 13.2 compares the useful temperature range and heat-load capacity of TECs to the corresponding values for other cooling methodologies. TECs are not recommended for use below 130 K because of their prohibitively low efficiencies. This recommendation is not a hard rule; it indicates that operation below 130 K is likely to be impractical but not necessarily implausible.

A major TEC issue is the structural integrity of bismuth telluride and soldered joints when subjected to differential thermal expansion stresses. Externally imposed stresses are commonly resolved through the inclusion of a compliant conductive strap on the cold side of the device. Compliant straps are generally fabricated of multiple layers of thin copper foil (2 mil is a common thickness); these straps typically are quite compliant along two axes and somewhat less so along the third. Another potential issue is redundancy, which can lead to increased complexity, larger heat loads, greater radiator area, and/or warmer rejection temperatures. TECs are fairly reliable; therefore, space applications have generally not flown redundant TECs.

### Characteristics

Figure 13.3 depicts actual and theoretical TEC performance characteristics and compares the performance of some TECs built for terrestrial in-vacuo applications. Some of the listed manufacturers are no longer actively producing and marketing TECs; still, this figure has been included to demonstrate general TEC performance

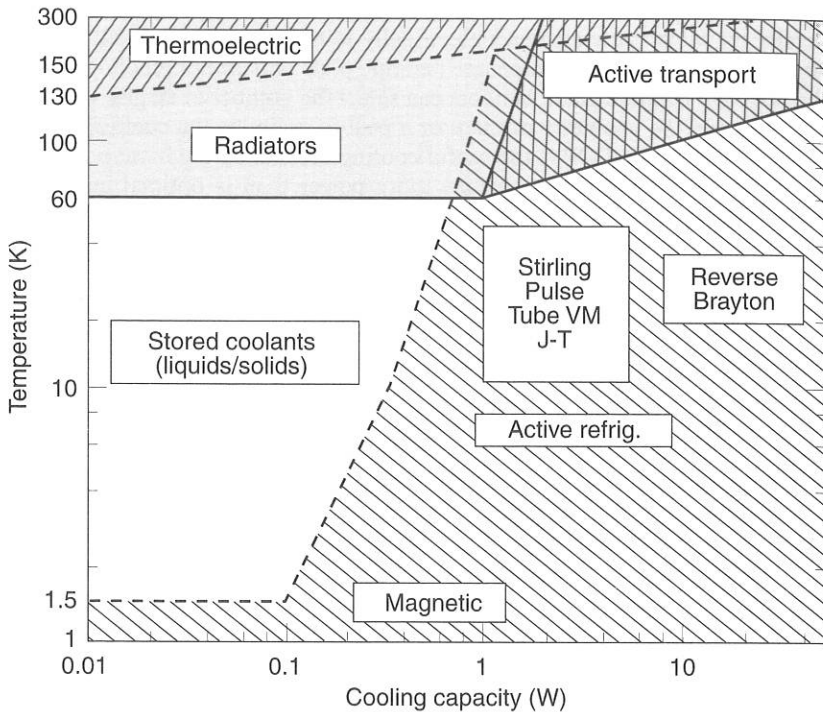


Fig. 13.2. TECs versus other cooling methodologies.

characteristics. The theoretical curve for 300 K shows that specific-power consumption increases very rapidly for colder cold-junction temperatures (typically doubling with each 10°C drop)—and this pattern does not factor in the increased parasitic cooling load. The performance of several of the units does not approach the theoretical performance limit (to the left of the 300 K curve). One point of reference shown by this chart is that at the theoretical performance limit, a TEC with a  $-54^{\circ}\text{C}$  cold side and a  $27^{\circ}\text{C}$  hot side needs 10 W of input power to produce 1 W of cooling.

Two other sources of readily available TEC performance information are the Web sites [www.marlow.com](http://www.marlow.com) and [www.melcor.com](http://www.melcor.com). These sites have a wealth of practical TEC information, as well as free downloadable cooler-sizing software. However, this information is generally limited to one- and two-stage TECs. Also, some advice on these sites may not necessarily be applicable to space systems.

### Optimizations

For space applications, the use of customized TECs is appropriate for optimizing the COP for the expected hot- and cold-side temperatures and heat flow. Not using an optimized TEC could increase power consumption as well as heat-rejection area, both generally valuable resources in spacecraft. Also, vendors can add robustness to custom TECs by physically enlarging the footprint of the upper

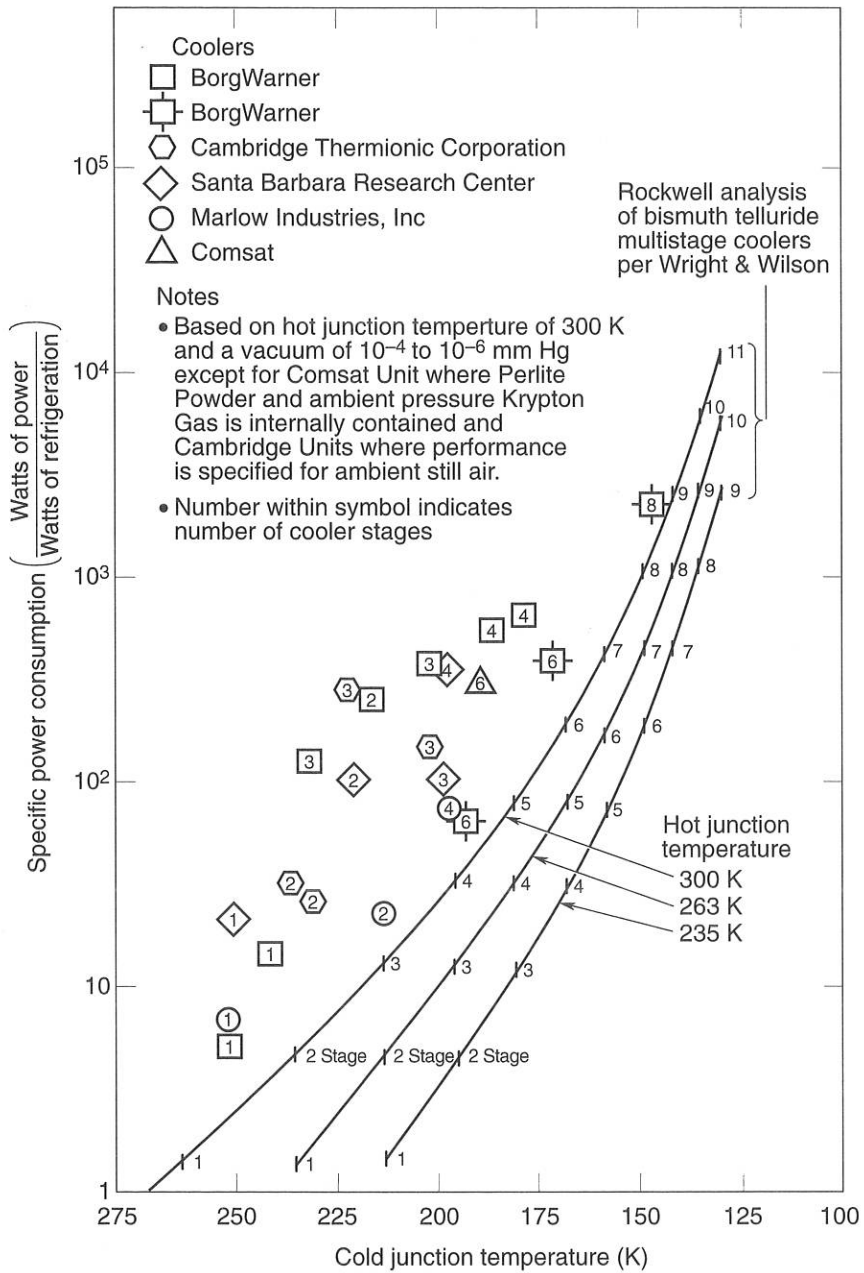


Fig. 13.3. Performance of TECs.

stage(s) and locating the majority of elements around the upper-stage periphery. Per the wedding-cake analogy, making a larger top layer with a hollow center can make the TEC stronger. In addition, a custom TEC can take advantage of an available spacecraft bus voltage, thereby avoiding any additional power conversion.

The ability to readily tailor the rejection temperature (by manipulating radiator parameters) offers control of a variable used in the overall system optimization. The system can be designed to optimize power, mass, and area according to spacecraft allocations and resource priorities. The hot-side temperature selection can trade the use of a larger radiator (i.e., a case in which the radiator operates at a lower temperature) for a more capable cooler (i.e., a case where the radiator handles higher dissipation at a higher temperature) for obtaining an efficient system.

### Heat Load Testing

In installations with significant uncertainty about the parasitic heat load, heat load testing is recommended. The test-article configuration can be simplified as long as it is thermally representative. An oversized "off the shelf" (but calibrated) cooler can be employed in determining heat loads. Such tests can use an oversized radiator and heater with dedicated power supply for independent hot-side temperature control. Alternatively a temperature-controlled heat sink can be used.

The potential for a "thermal runaway" condition, which may arise from constrained applications such as limited radiator area, may be staved off by reducing the thermal resistance between the TEC hot side and the heat sink. Thermal runaway, explored in the application example below, is a condition in which temperature rise at the radiator necessitates an increase in drive power to the TEC, thus causing a further rise in temperature at the radiator, and so on.

### Interfaces

A paramount design detail for TEC integration is an efficient heat-transfer path at the cooler interfaces that does not induce mechanical failures. Differences in coefficient of thermal expansion (CTE) between the TEC substrate and mating surfaces can cause internal stresses, fatigue, and failure. The construction of TECs and their associated fragile nature make their mounting extremely difficult. Traditionally, they are bonded or clamped. In the first case, a controlled and effective bondline may have a high inherent resistance, and in the second, the clamping may give rise to high local mechanical loads, variable resistance from assembly to assembly over time, and the need for coupling compound. Certain low-heat-load and low-watt-density installations can effectively employ a pliable interface material to minimize stress resulting from the temperature-induced differential expansion. However, pliable interface compounds are low-conductance phenolics that can yield significant gradients, which then would need to be overcome, hence further taxing the TEC. Often, both approaches prove impossible to use in a contamination-sensitive context, such as a location close to optical detectors.

However, for a ceramic-substrate TEC to be manufactured, the substrates are metallized. This process can also be productively utilized on the hot and cold interfaces to provide a surface receptive to a solder joint. This joint must, of necessity, be made after the TEC itself has been manufactured and tested; in addition



the soldering temperature must be lower than that used in the TEC assembly process itself. TEC manufacturers commonly anticipate this approach and use the highest-temperature solder possible consistent with their manufacturing process. Nevertheless the purchaser of a high-performance, high-cost TEC is advised to engage the manufacturer in the mounting process to avoid accidental internal damage or degradation during TEC soldering into the mounts.

Mounts should be of a relatively close match in terms of CTE to the TEC substrate. Alumina, a common TEC substrate, has a CTE of  $7 \times 10^{-6} \text{ K}^{-1}$ , which is considerably lower than that of conventional spacecraft materials (e.g., aluminum) downstream from the TEC hot side. One potential CTE mismatch solution involves an intermediary beryllium sink, which better matches the TEC substrate CTE. Again, hard materials may cause thermal-resistance problems at joints, and further metallurgical (soldering or brazing) joining techniques may be indicated.

### XRT Focal-Plane TEC Mounting

In accordance with this design philosophy, the TEC for the Swift X-Ray Telescope (XRT) focal-plane camera assembly employed two metallurgical joints (copper/beryllium solder and beryllium/aluminum alloy braze) resulting in a tenfold thermal-conductance improvement over a bonded system. This improvement reduced the peak  $\Delta T$  requirement on the TEC by 10 K. The corresponding reduction of power dissipated may be estimated from the TEC power characteristic shown in Fig. 13.4.

Figure 13.5 is a photo of the flight model Swift XRT focal-plane camera-assembly CCD mounted on the cold side of the TEC. The hot-side mounting details may be discerned, along with the provision for strain-relieved electrical wiring (note the gauge of the wire). The aluminum alloy base is 40 mm on a side; this measurement conveys the scale of the image. Also, note the appearance of the upper stages of the TEC in the highly reflective baseplate.

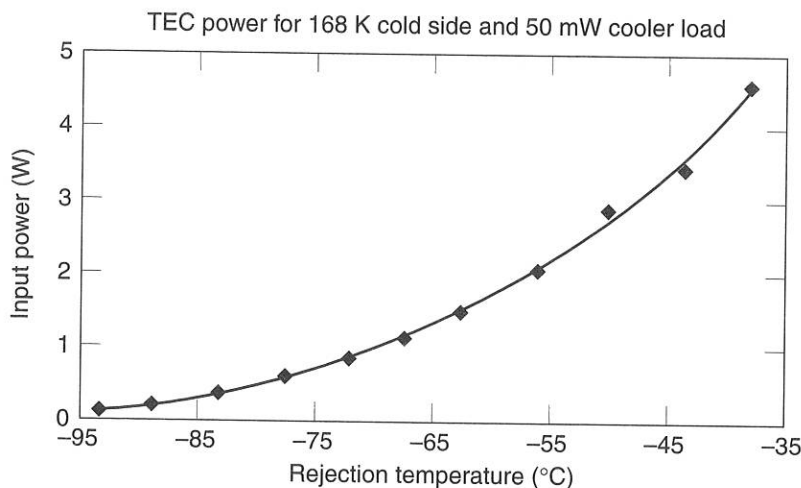
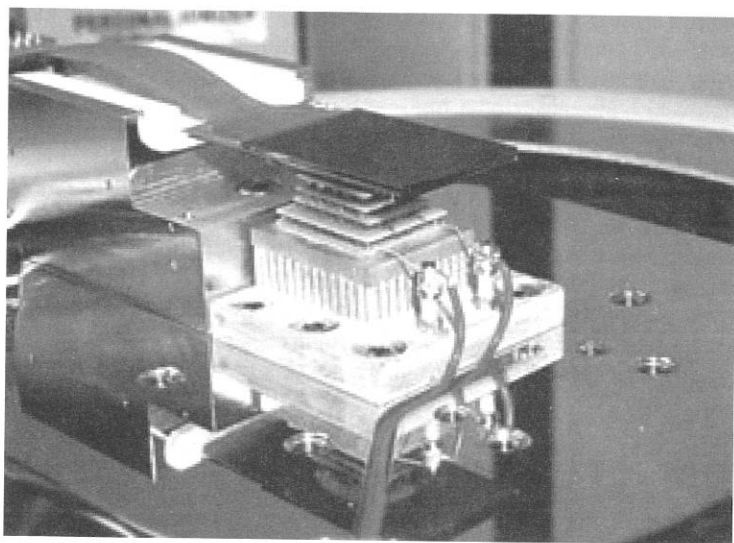


Fig. 13.4. TEC performance data from XRT development program (courtesy of University of Leicester, United Kingdom).



**Fig. 13.5.** Swift XRT CCD integrated with TEC and heat sink (photo courtesy University of Leicester).

### Design Development

Decisions regarding the number of stages, the number of junctions per stage, and the like should be left to the TEC vendor. The TEC end user, however, needs to be aware of how such decisions can affect performance and margins. Adding more stages than are optimal will generally depress efficiency. Demanding a cooling load that is greater than optimal can make a TEC operate in an inefficient regime. As a general rule, TECs with fewer stages offer the potential for greater cooling-load margin while TECs with more stages offer the potential for greater temperature margin. Sharing uncertainties and margin preferences with the TEC vendor could result in a better-suited TEC—particularly in regimes where discretion can be exercised with respect to number of stages.

Clearly, prediction of TEC performance is critical to early design decisions. Prediction invariably requires the involvement of the TEC vendor, because the thermoelectrical coefficients are a function of materials and construction, and they are often proprietary. This modeling effort is a standard service that is part of the custom device development, and it gives some confidence that what is being offered is optimal for the application. Despite the apparent precision of TEC mathematical modeling, procurement of a prototype early in the design process for the heat-rejection system is strongly advised. Testing this prototype will allow subsequent steps to take place in a timely fashion—more precise sizing of other thermal components, trials on jointing techniques and their qualification, and development of the electrical control system (a step that is crucial to avoiding thermal runaway).



### Power Supply

Stable dc voltages with pulse-width modulated power supplies are recommended for TECs. Particularly in optical systems, where outgassing constituents are most likely to collect on the coldest local object, it may be appropriate for the TEC power supply to have a reverse-power mode for heating and driving contaminants from the optical sensor. A smart power supply may be employed in situations where limiting thermal runaway is warranted.

### Application Example

In 1986, the RCA Satcom Ku-band spacecraft was launched into geosynchronous orbit with a cooled low noise amplifier (CLNA) operating at  $-50^{\circ}\text{C}$  for improved uplink receiver performance. Uplink signals reaching geosynchronous satellites are very weak because of the long transmission distance and the fading that results from atmospheric effects. Receiver signal quality is improved by operating the initial amplifier stages at this cold temperature, where the largest source of noise, "thermal noise," is suppressed.

Figure 13.6 depicts the heat flow and energy balance for the heat pump and amplifier. The TEC uses the Peltier effect to pump heat from the cold side (amplifier) to the hot side (radiator). The TEC pumps amplifier dissipation and any parasitic heat through a compliant conductive strap; this heat, as well as the TEC input power, is conducted to the local radiator, where the heat is rejected to space. The conductive strap provides a mechanically compliant heat path that relieves stresses from induced differential thermal expansion. The cooler's remote power-supply unit, the TEC controller (TECC), monitors the amplifier's temperature and modulates cooling power, thus maintaining the amplifier temperature at  $-50 \pm 1^{\circ}\text{C}$ .

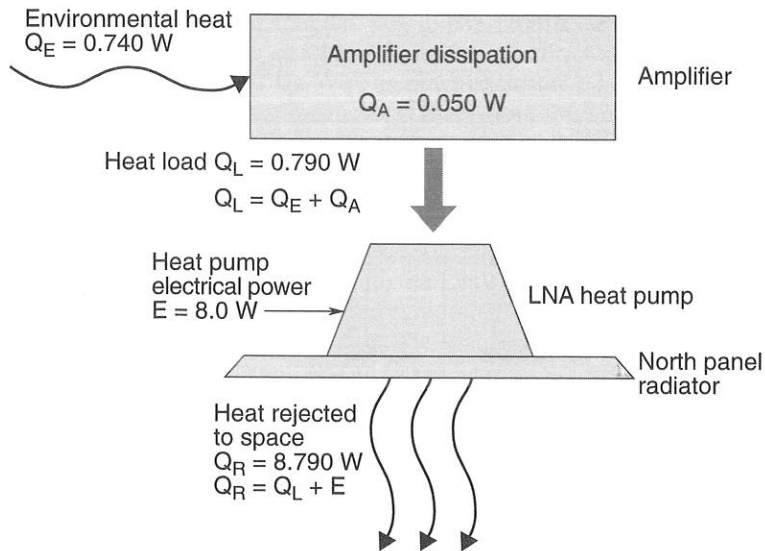


Fig. 13.6. TEC and amplifier energy balance and heat flow.

### General Configuration

Figure 13.7 depicts the general configuration and thermal features of the CLNA assembly. The waveguides, which serve as the input and output RF (radio-frequency) path, suspend and thermally isolate the LNA within the enclosure. The LNA is conductively coupled via the compliant strap to the TEC's cold side. The CLNA enclosure is formed of a low-emittance aluminum foil bonded with a conductive adhesive to the CLNA assembly spreader plate and top plate. The foil also serves to attenuate noise. The aluminum legs form the primary conductive coupling from the top plate to the spreader plate; they typically keep gradients between the top plate and spreader plate less than  $2^{\circ}\text{C}$ . For heat rejection, the CLNA assembly is mounted onto, and is in intimate thermal contact with, the satellite's north radiator panel.

### Thermal Design Development

The thermal design goal was to produce a stable  $-50^{\circ}\text{C}$  operating environment for the LNA without substantial increase in system weight, power consumption, or risk. To meet this goal, development efforts concentrated on reducing the LNA parasitic heat loads, quantifying the cooling requirement, specifying an optimum TEC, and sizing its radiator.

#### *Plastic Waveguide*

The largest initial amplifier heat load was via the waveguide. Conventional satellite waveguides are fabricated of 30-mil (or thicker) aluminum, a highly conductive material. It became obvious that the waveguide conductive path needed to be nearly eliminated. Conduction through polymer is typically three orders of magnitude lower than that through aluminum. A competing requirement was that this waveguide also be electrically conductive, to channel RF signals. So a highly insulating polymer waveguide with a vapor-deposited thin metal was developed. A

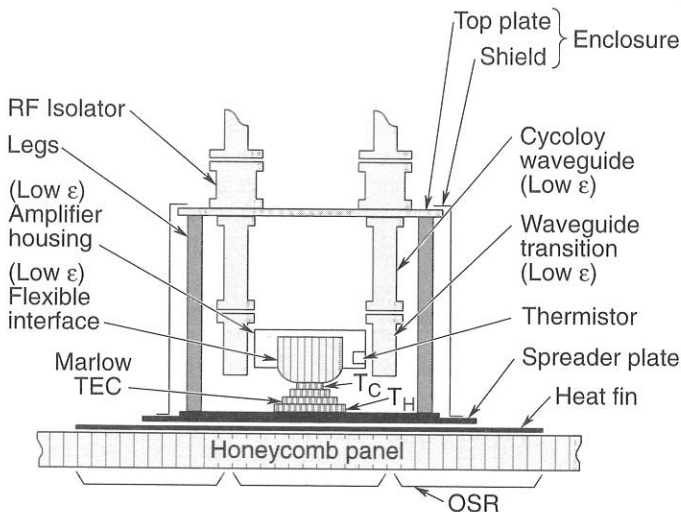


Fig. 13.7. LNA and enclosure.

polycarbonate, Cycloy, was selected for its combination of mechanical and thermal properties—low outgassing, machinability, and affinity for thin plating (the last an especially desirable property). The Cycloy waveguides have a vapor-deposited thin metal coating on the interior and flange surfaces that renders the waveguide electrically conductive without substantially affecting its ability to serve as a thermal isolator.

#### *Miscellaneous Details*

To minimize radiative heat absorbed by the amplifier, the LNA used surfaces of low emittance throughout. The amplifier's 32-gauge electrical leads were chosen to minimize heat leak down the lead without compromising structural integrity.

#### *Compliant Conductive Strap*

The purpose of the compliant strap was to provide mechanically compliant heat transport between the TEC and LNA with a modest temperature gradient. The strap was similar in concept to other mechanically compliant thermal links, with stacked layers of metal curved to provide virtually no resistance to small displacements in two planes. The strap departed from the usual mechanically compliant thermal links in three ways. First, it was constructed of silver rather than copper. Silver is lighter and imparts lower loads to the TEC during vibration. Second, to eliminate interlayer gradients, the silver layers were fused to each other, but only in the vicinity of the cooler and LNA interfaces. Third, to reduce the TEC-to-strap gradient, the strap was permanently bonded to the TEC with a conductively loaded adhesive.

#### *Aluminum Enclosure*

The decision to set the local radiator operating temperature to a maximum of 15°C (as discussed below) clarified the advantage of creating an enclosure around the CLNA assembly. The initial thought was to use multilayer insulation (MLI) to form an effective barrier to radiation from the satellite's interior environment (which can be as warm as 30°C). With an outer enclosure conductively tied to the local radiator, LNA radiative parasitic heat loads from the surrounding spacecraft would be further reduced. The low-emittance aluminum-foil enclosure therefore would shunt spacecraft ambient radiation energy directly to the radiator and would surround the LNA in a 15°C cavity.

#### *Radiator Sizing Criticality*

The primary parasitic heat flow path into the LNA is radiation from the enclosure and conduction down the leads and waveguides. Because the enclosure temperature is quite close to that of the radiator, the heat flow (and therefore the cooling requirement) is directly proportional to the radiator temperature. If the enclosure (or radiator) temperature increases, the cooler has to work harder, thereby raising the radiator temperature. With this radiator-cooler relationship, the sizing of the radiator is critical, and undersizing it could lead to a thermal runaway condition in which additional power supplied to the cooler causes the cold area to be warmer.

### Cooler Heat Load Determination

To size and specify the cooler, we first determined the cooler heat load. Initial analysis predicted 525 mW. Because of the low efficiency of TECs, even small errors in estimating this value would translate into significant errors in the cooler waste heat and necessary radiator size. Therefore, the cold-side heat load was determined experimentally, as a function of the cooler's hot-side temperature. A series of calorimetric tests was conducted with a thermally representative CLNA assembly and a calibrated oversized TEC rejecting heat to a temperature-controlled heat exchanger. These tests established the cooling requirement to maintain the LNA at  $-50^{\circ}\text{C}$  for a range of baseplate temperatures ( $27$ ,  $15$ , and  $0^{\circ}\text{C}$ ). The net cooling was deduced from the measured power and the calibrated cooler performance curves. Sensitivity of the amplifier heat load to hot-side temperature is shown in Fig. 13.8. Because experimental values were more conservative than the analytical values, they were used for cooler selection and radiator sizing.

### Selection of Rejection Temperature

Rejection temperature was the final parameter needed to design and build an optimized cooler. This temperature affects both the specification (and therefore the optimization) of the TEC and the local radiator sizing. Selecting an excessively cold rejection temperature would result in a large and heavy radiator, while an excessively warm rejection temperature would cause the TEC to consume excessive power, resulting in inappropriate use of radiator area. The selection needed to be a compromise between radiator area (a warmer rejection temperature would be needed for a smaller area) and power consumption (a colder temperature would be needed for lower power). Optimal rejection temperature would balance TEC power consumption against radiator area.

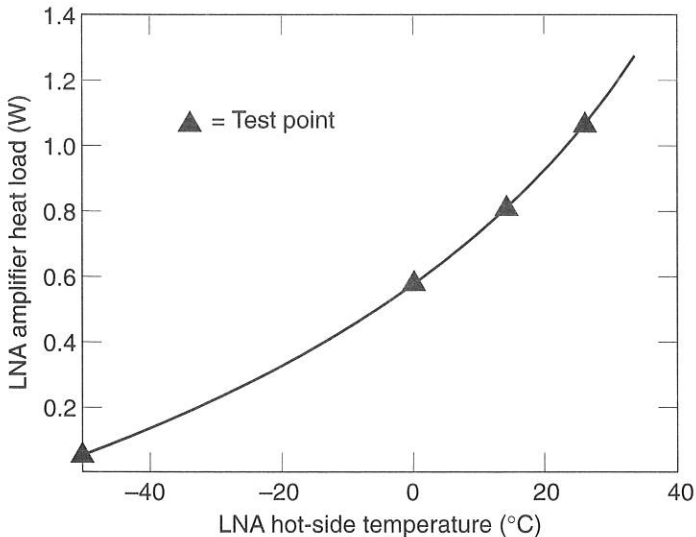


Fig. 13.8 LNA amplifier heat-load dependence on hot-side temperature

We first looked to establish the minimum possible range of radiator temperatures by determining the effect of external equivalent sink temperature and the internal environment on the radiator. The external equivalent sink temperature is a single sink temperature that is equivalent to the environmental flux (solar flux), radiative interchange with other bodies (13% worst-case view to solar array at 50°C) and surface-finish parameters (absorptance and emittance). In calculations or in IR testing, using an equivalent sink causes the object in question to run at the same temperature as it would with all those external fluxes and parameters imposed. The external equivalent sink temperature was calculated to be -16°C using Eq. (13.1):

$$T_{\text{ext eq sink}} = [(\alpha/\epsilon \cdot S \sin(\theta) + F_{\text{array}}\sigma T_{\text{array}}^4)/\sigma]^{1/4}. \quad (13.1)$$

This calculation assumes an OSR solar absorptance ( $\alpha$ ) of 0.25, emittance ( $\epsilon$ ) of 0.80, solar constant ( $S$ ) of 0.135 W/cm<sup>2</sup>, incident solar angle ( $\theta$ ) of 23.5 deg, worst-case view factor to the solar array ( $F_{\text{array}}$ ) of 13%, and solar array temperature ( $T_{\text{array}}$ ) of 50°C. The Stefan-Boltzmann constant ( $\sigma$ ) is  $5.67 \times 10^{-8}$  W/m<sup>2</sup>·K<sup>4</sup>.

The local internal temperature ( $T_{\text{int}}$ ) can be as warm as 30°C. The sum of the internal and external equivalent sinks (per Eq. [13.2]) represents the net equivalent sink for the CLNA radiator. The low-emittance irridite surface finish ( $\epsilon_{\text{int}} = 0.11$ ) was selected for the radiator interior surface to minimize radiant heat absorbed from the spacecraft interior, thereby allowing the CLNA radiator to achieve colder temperatures. The net effective sink (considering both internal and external environments) is -9°C:

$$T_{\text{net eq sink}} = [(\epsilon T_{\text{ext eq sink}}^4 + \epsilon_{\text{int}} T_{\text{int}}^4)/(\epsilon + \epsilon_{\text{int}})]^{1/4}. \quad (13.2)$$

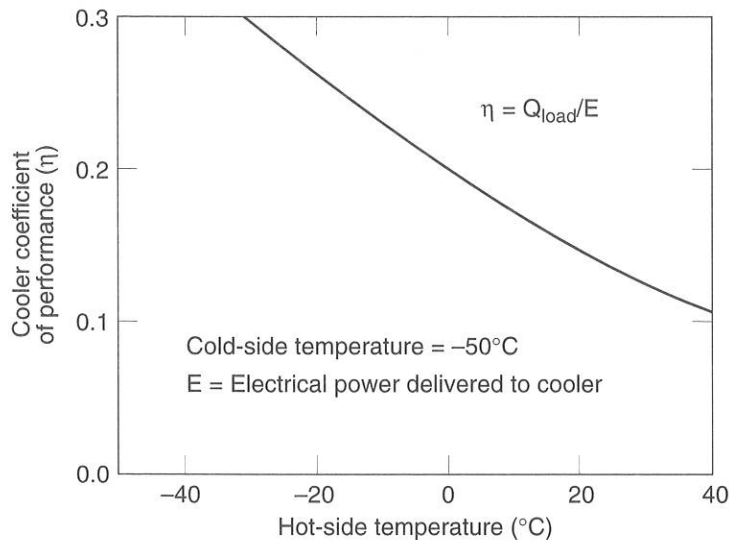


Fig. 13.9. Estimated theoretical limit of cooler performance.

This calculation indicates that even with an infinitely efficient TEC, the CLNA radiator could not operate at a temperature of  $-9^{\circ}\text{C}$  or below. Thus the cold bound of plausible rejection temperatures was established.

To compare various rejection temperatures, we needed heat-pump performance for various hot-side temperatures and  $-50^{\circ}\text{C}$  for the cold side, but this data was not directly available. TEC manufacturers typically evaluate and publish performance data with the cooler hot side at  $27^{\circ}\text{C}$ . We estimated this performance curve using published TEC performance curves and a performance-equivalence transform suggested in the cooler-sizing guide published by Marlow Industries, Inc.<sup>13.1</sup> The transform indicates that for a given power, reducing the hot-side temperature by  $3^{\circ}\text{C}$  reduces cold-side temperature by  $1^{\circ}\text{C}$ . The resulting transformation and interpolation yielded Fig. 13.9, which represents the estimated theoretical limit of cooler performance for the cold side at  $-50^{\circ}\text{C}$ . Each incremental point on the curve represents an optimized cooler for that particular hot-side temperature. Hence this curve represents an optimistic bound on performance.

Using a spreadsheet is a straightforward means to establish TEC power consumption and radiator area required over the range of plausible rejection temperatures. The TEC cooling load (Fig. 13.8) and COP (Fig. 13.9) can be represented by equation or table. Dividing the heat load by the COP gives the TEC power consumption. Table 13.2 indicates that the power continues to increase with temperature. The area is calculated using radiation heat-transfer equations and appropriate couplings to both space and the spacecraft interior. For this application, the spreadsheet indicated a range of reasonable solutions with the radiator temperature between  $5^{\circ}\text{C}$  and  $30^{\circ}\text{C}$ . A design hot-side temperature of  $15^{\circ}\text{C}$  was selected as a compromise between low input power and radiator area.

The TEC vendor was given the following parameters: 790 mW cooling requirement,  $-52^{\circ}\text{C}$  cold-side temperature (allowing for a  $2^{\circ}\text{C}$  gradient in the strap), and  $+15^{\circ}\text{C}$  hot-side (rejection) temperature. The vendor's optimization indicated that a four-stage cooler would consume 8 W of power.

**Table 13.2. Radiator Sizing Summary**

$T_{\text{radiator}} (^{\circ}\text{C})$	Theoretical Input Power	
	(W)	Area ( $\text{cm}^2$ )
-5	2.5	2023
0	3.0	1005
5	3.5	732
10	4.1	610
<b>15</b>	<b>4.9</b>	<b>545</b>
20	5.7	509
25	6.7	491
30	7.9	485
35	9.4	490
40	11.2	506



### *Radiator Sizing*

The final design step was to size the CLNA radiator, using the 8 W input power plus the 0.79 W heat pumped, and an assumed 0.80 fin effectiveness. Radiated heat from internal and external sources was covered by virtue of using the equivalent sinks. Heat conduction along the waveguide external to the CLNA assembly was erroneously neglected, but that condition was probably more than offset by improvements to the surface finishes and enclosure. The required radiator area was 0.106 m<sup>2</sup>.

### **Test Results and Flight Data**

A test of the final CLNA configuration was performed with an engineering model CLNA bolted to an equivalent aluminum plate representing the radiator panel. This test demonstrated adequate cooling and radiator-area margin. The CLNA operation was as expected during spacecraft thermal-balance testing, which simulated the worst hot expected flight environment. Initial flight data also indicated that the CLNA was properly maintaining the LNA at -50°C.

### **Reference**

- 13.1. Marlow Industries, Inc., "A Guide to Thermoelectric Heat Pumps," Catalogue No. 98-002.